Bioimages 14 : 9-18, 2006.

Quantitative Analysis of Photodamage During Fluorescence Bioimaging: Monitoring of Nitric Oxide Production using DAF-2

Takashi Kuroda[1], Yoh-ichi Satoh[1]*, Hitomi Akutsu-Yamauchi[1], Yuuki Shikanai[1], Setsuya Miyata[1], Tomoyuki Saino[1], Denis Russa[1], Yoshiaki Habara[2], Zon-Jie Cui[3]

[1]Department of Histology, School of Medicine, Iwate Medical University, Uchimaru 19-1, Morioka 020-8505, Japan, [2]Laboratory of Physiology, The Graduate School of Veterinary Medicine, Hokkaido University, Sapporo 060, Japan and [3]Institute of Cell Biology, Beijing Normal University, Beijing 100875, PR China

Summary

Photodamage occurs, to a greater or lesser extent, during fluorescence bioimaging, and various procedures are empirically used to reduce the extent of this damage. However, measuring photodamage is difficult. Nitric oxide (NO), a gaseous messenger, is a free radical, and can be induced by light-exposure. In the present study, NO production was determined by the treatment of cultured cardiomyocytes, hippocampal neurons, dorsal root ganglion cells and serous peritoneal mast cells with 4, 5-diaminofluorescein (DAF-2). During laser irradiation in confocal microscopy, the fluorescence intensity of DAF-2 was increased in many punctuate regions of the cytoplasm as well as the nuclei of the cells examined. After the increase in NO levels, the beating of cardiomyocytes and the exocytosis of mast cells ceased. A stronger laser power caused a more intense peak and a more rapid increase in NO production. NO production in mast cells under various conditions was observed, in an attempt to reduce the extent of photodamage. Intermittent irradiation had no effect on NO production. Antioxidants (bovine serum albumin, vitamin E and melatonin), inhibited the peak and delayed the time course for NO production at a weak laser power, but had no effect on the bleaching of Indo-1, a fluorescent calcium indicator. In all bioimaging experiments in which a fluorescence technique is involved, the possibility of photodamage should be considered, and monitoring NO production by DAF-2 continues to be a relatively straightforward method for detecting photodamage.

Key words

Nitric oxide, DAF-2, photodamage, monitor, antioxidants

Introduction

Bioimaging techniques using fluorescent probes in living cells are in widespread use in the field of cell biology. The technique permits real-time changes in intracellular calcium ion concentration ($[Ca^{2+}]_i$) (Berridge et al., 2003), various phosphorylation processes (Nahorski et al., 2003) and cell organelle trafficking (Kawata et al., 2001; Waguri et al., 2003) to be observed. However, ultraviolet~blue light or laser which are typically used in fluorescence bioimaging can be harmful to living cells, and an intense laser, which is used in confocal microscopy, may have an effect on cellular processes by producing free radicals (e.g., reactive oxygen, nitric oxide). Some photosensitive substances in the cells modulate physiological Ca^{2+} responses; photodynamic action (Cui et al., 2000, 2002). Although photodamage or photodynamic action in bioimaging has been empirically discussed in various meetings and symposia, only a few studies have reported on the monitoring or an assessment of whether light or laser has an effect on the responses.

Nitric oxide (NO) is a gaseous transmitter produced in living tissues, and plays multiple roles in both intracellular and extracellular signalling mechanisms with implications in health and disease. NO may be produced during fluorescence bioimaging, resulting in photodamage. NO production is typically evaluated by the presence of NO-synthase or reactive products (e.g., nitrite and nitrate) (Preiser et al. 1996), but these methods are either prospective or retrospective, and it is difficult to monitor the NO production in real-time. A specific fluorescent NO probe, 4, 5-diaminofluorescein (DAF-2), was recently developed (Kojima et. al., 1998), in which the increase in fluorescence intensity of the dye serves as an indicator of NO produced. Such a dye should be useful in analyzing the real-time production of NO in living cells.

*To whom all correspondence should be addressed.
E-mail: yisatoh@iwate-med.ac.jp

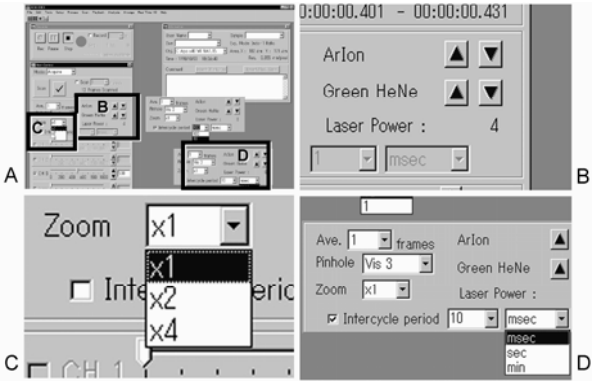

Fig. 1. Control panel of a confocal microscope, RCM/Ab. (A) Graphic user-interface of RCM/Ab. (B) The laser power of argon-ion laser and green HeNe laser was controllable, but the numerical value of the laser power did not reflect the absolute energy. (C) When the optical zoom was set at ×2 or ×4, the laser intensities at the specimen increased 2 or 4 times, respectively. (D) Image acquisition time interval could be set *ad libitum* (1 ms−1,000 min)

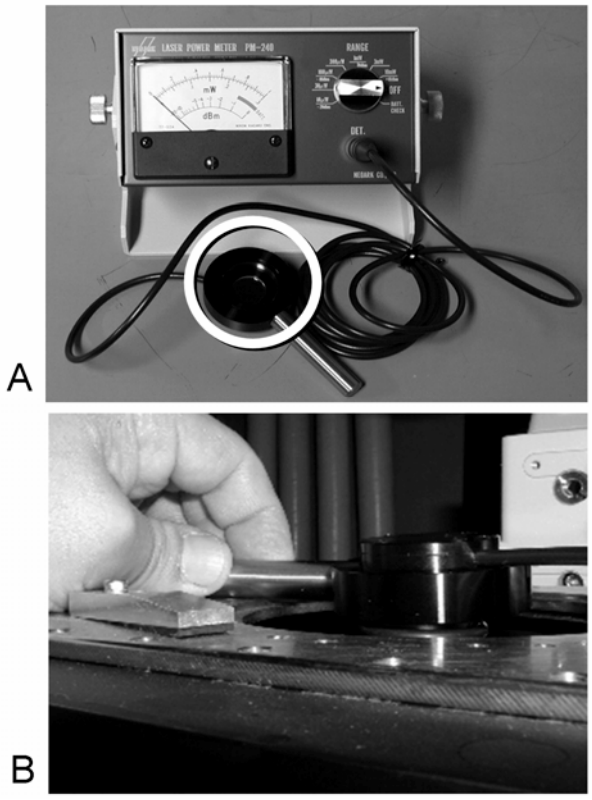

Fig. 2. Laser power meter. (A) PM-240. The laser detector is circled. (B) The detector was located on the objective lens, and adjusted at the focal plane.

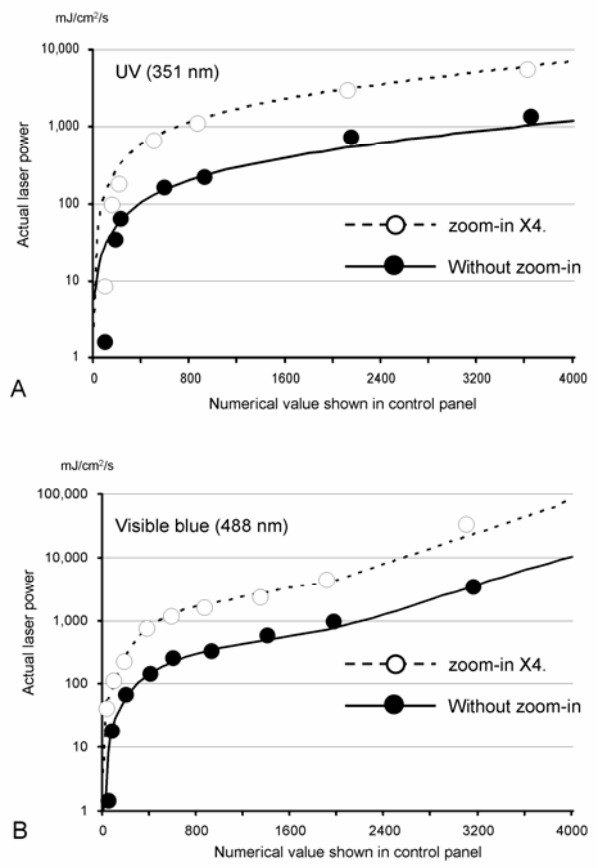

Fig. 3. Graphs showing correlations between the actual laser power and the numerical value shown in the control panel. (A) UV laser (351 nm). (B) Blue laser (488 nm). Solid circles and solid lines: actual measurements and values estimated by an equation without optical zoom-in. Open circles and dotted lines: actual measurements and equation values at optical zoom-in ×4.

The quantification of photodamage is important in terms of reducing artifacts that might be produced during fluorescence bioimaging. NO production in living cells may be an objective indicator of photodamage. In the present study, we observed the fluorescence intensity of DAF-2 during fluorescence bioimaging by confocal laser scanning microscopy in real-time. In addition to photodamage, fluorescent dye-bleaching is a serious problem in bioimaging. For example, due to its rapid bleaching, Indo-1 is not commonly used in bioimaging to analyze intracellular calcium ion concentrations ($[Ca^{2+}]_i$), although the dye permits the quantitative determination of $[Ca^{2+}]_i$ and is generally considered to be an ideal dye for measuring rapid changes in $[Ca^{2+}]_i$. The issue of whether anti-oxidant substances are effective in inhibiting NO production and dye-bleaching was also examined.

Materials and Methods

Cell specimens

Cardiomyocytes and hippocampal neurons were obtained from embryonic or neonatal rats and then maintained in culture (Konno et al., 2002; Miyata et al., 1996). Dorsal root ganglia were obtained from adult golden hamsters (body weight 100–120 g), and the connective tissue removed by digestion with collagenase (Type II, 100 U/ml, 37°C for 40 min) to obtain isolated nerve cells. Peritoneal serous mast cells were collected from adult rats (Wistar, body weight 200–300 g) (Mori et al., 2000).

Dye loading

DAF-2 was used to detect NO production. NO converts DAF-2 to DAF-2T, which emits bright fluorescent light (Ex; 495 nm, Em; 515 nm). As a result, the increase in fluorescence is proportional to NO production. Dichlorofluorescein (DCF) (Ex; 510 nm, Em; 534 nm) was used to determine the concentration of intracellular free radicals (e.g., superoxide, nitric oxide) and/or reactive oxygen species (e.g., hydrogen peroxide). To examine the effect of antioxidants on the bleaching of the fluorescent dye, Indo-1 (a UV-excited calcium indicator, Ex; 346 nm, Em; 401–475 nm) was loaded to cells.

The effect of photodamage on the secretory mechanism was estimated. Mast cells were loaded with Fluo-3 (a calcium indicator, Ex; 506 nm, Em; 526 nm), and sulforhodamine-B (SFRM-B, Ex; 565 nm, Em; 586 nm, 50 μg/ml) in perfused HEPES-buffered Ringer solution (HR; composition described below) was added, to visualize exocytosis. Exocytosed granule matrices are strongly stained by SFRM-B and fluoresce strongly (Mori et al. 2000). The cells were stimulated by treatment with compound 48/80, which activates the G-protein of the cells.

The cells were incubated in HR for 40–60 min at room temperature (approximately 25°C) containing lipophilic ester derivatives of the dyes, DAF-2/DA (2–10 μM) , DCF/AM (2–5 μM), Fluo-3/AM (2 μM), Indo-1/AM (2–5 μM). These entered the cells through the plasma membrane, and were cleaved by endogenous esterases, releasing the NO/free radical- or Ca^{2+}-sensitive form of the indicators intracellularly. DAF2-DA was purchased from Daiichi Pure Chemical (Tokyo, Japan), SFRM-B from Invitrogen-Molecular Probes (Eugene, OR, USA), and Indo-1/AM and Fluo-3/AM from Dojindo (Kumamoto, Japan).

Confocal microscopy

A real-time confocal microscope (RCM/Ab; revised version of RCM-8000, Nikon, Tokyo, Japan) was used to determine intracellular NO and/or exocytosis of mast cells. An argon laser (Enterprise II 621; 351–364 nm and 480 nm; Coherent, Santa Clara, CA, USA) and a HeNe laser (25-LGR-193; 543 nm; Melles Griot, Carlsbad, CA, USA) were attached to an inverted microscope (TE 300, Nikon), and fluorescence emission was guided through a water immersion objective lens (C Apo 40×, NA 1.15, Nikon) to a pinhole diaphragm. The laser power, optical zoom, interval of intermittent image-acquisition and other parameters were adjusted using the control panel of the system (Fig. 1).

Cells loaded with DAF-2 were exposed to a blue laser (488 nm) to measure NO or related free radical production, respectively. To examine photodamage on the exocytotic mechanism, some mast cells were loaded with Fluo-3 and immersed in HR containing SFRM-B. To evaluate the effect of antioxidants on photobleaching, mast cells loaded with Indo-1 were exposed to an ultraviolet laser (351 nm).

The numerical value of laser power shown in the control panel (Fig. 1B) indicated only relative value of laser power at the ND filter at the scanning unit, but not the absolute value at the specimens. Therefore, we measured the actual energy transmitted through the objective lens by a laser power meter, which was silicon type (Power Joule Meter PM-240, Neoark, Tokyo, Japan; Fig. 2) at different numerical values in the control panel. The direct detective wavelength of the meter was 632.8 nm. When the power of visible-blue or UV laser was measured, it was necessary to multiply by a coefficient. The power of the blue laser (488 nm) was corrected by a coefficient for 488 nm. To estimate the power of the UV laser (351 nm), coefficient for 442 nm was applied, therefore the values for the UV laser power were not accurate, but relative and rough. The detector was set at the cover-glass level, although the focal plane for living cell imaging was more or less higher than the cover-glass.

Perfusion

The cells were continuously perfused with the standard HR (1 ml/ min) at room temperature. The extracellular bathing HR solution contained (concentration in mM): NaCl 118, KCl 4.7, $CaCl_2$ 1.3, $MgCl_2$ 1.1, NaH_2PO_4 1.0, glucose 5.5. In addition, MEM amino acid solution (Gibco, Grand Island, NY, USA) and 2.0 mM L-glutamine and 10 mM HEPES were added. The solution was adjusted to a final pH of 7.4 with NaOH, and equilibrated with 100% O_2.

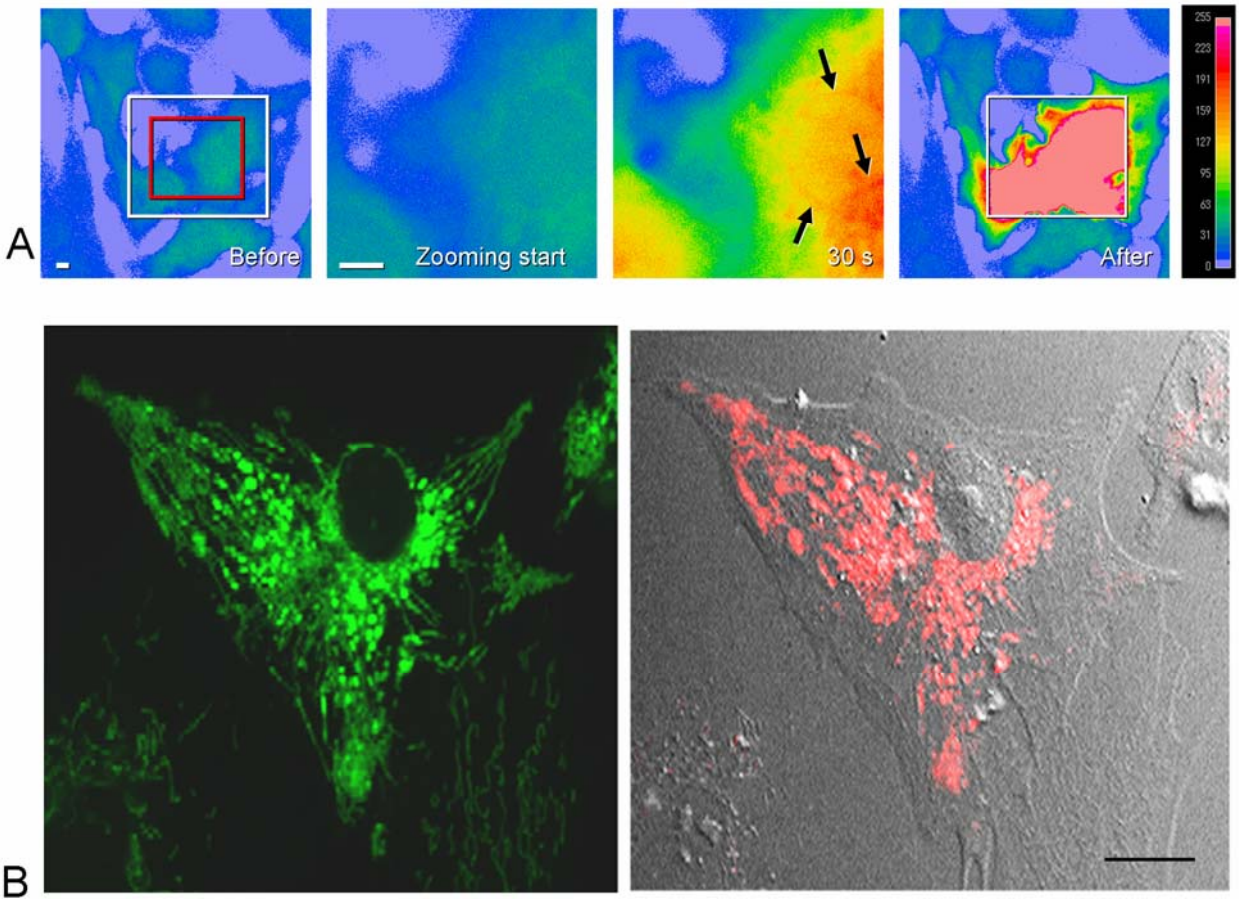

Fig. 4. Cultured cardiomyocytes showing NO production. (A) Pseudocolor images showing the fluorescence intensity of DAF-2. Cardiomyocytes irradiated by a blue laser (488 nm). Zoom-in (×4) increased laser energy at the specimen (300→1200 mJ/cm^2/s), and the fluorescence intensity then increased. The irradiated region at zoom-in is outlined by a white rectangle. In this microscopy, zoom-in images (outlined by red rectangle) were smaller than the irradiated area. Note the thread-like structures (arrows). Bar: 5 µm. (B) Fluorescence image of DAF-2 (left; green) and differential interference contrast and fluorescence image of Mitotracker (right; red). Bar: 10 µm.

After a brief washing with the HR, the specimens were continuously perfused with HR containing the following substances: compound 48/80 (a stimulant of mast cell exocytosis; Sigma-Aldrich, MO, USA; approximately 10 µM), 200 µM vitamin E (α-tocopherol; Sigma-Aldrich), 10 µM melatonin (Nacalai Tesque, Kyoto, Japan) and/or 5% bovine serum albumin (BSA; Sigma-Aldrich).

Results

Monitor of laser power

The laser energy through the objective lens was measured (Fig. 2), and these values are depicted (Fig. 3; circles). Based on the results, equations were constructed using the Excel graph wizard (lines in Fig. 3). In both UV and blue laser, no simple linear correlation was found between the numerical value shown in control panel and the laser power. The energy of the laser was estimated following the equation.

Based on the equation, we calculated the approximate laser energy used in routine work in our laboratory; for physiological studies, ca. 20–200 mJ/cm^2/s (UV laser) and 60–400 mJ/cm^2/s (blue laser), and in some cases, an intense laser (>1000 mJ/cm^2/s) is used for morphological observations. However, in bioimaging, various substances (e.g., immersion solution, cover-glass, perfusion solution and cells/tissues) intervene between the objective lens and the focused cells. Obviously, distance as well as intervening substances affected the actual laser energy at the specimen, but it was not possible to determine this with any degree of accuracy.

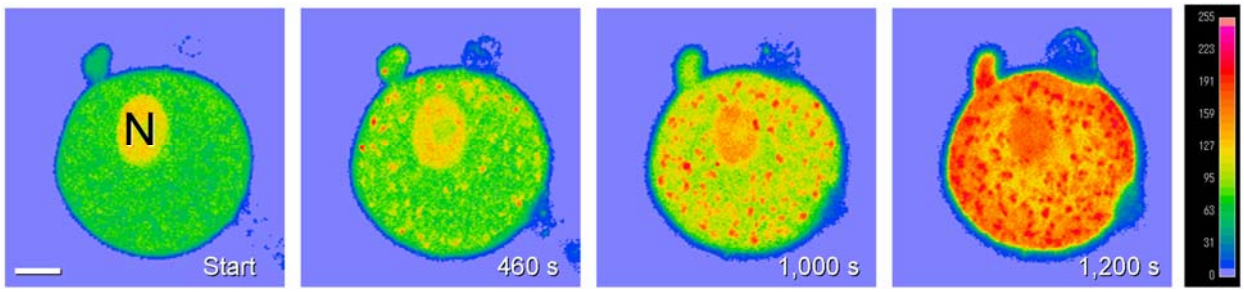

Fig. 5. An isolated neuron from a dorsal root ganglion showing NO production. Pseudocolor images showing the fluorescence intensity of DAF-2. The cell was irradiated by a blue laser (488 nm; 7,700 mJ/cm^2/s). The increase was spotty. N: nucleus. Bar: 10 μm.

Cardiomyocytes

Cultured cardiomyocytes contracted periodically in the perfusion chamber under the conditions of confocal microscopy. The DAF-2 fluorescence intensity was weak during continuous blue laser irradiation (about 300 mJ/cm^2/s). However, when zoom-in images were obtained (about 1,200 mJ/cm^2/s), the DAF-2 intensity in the cells increased and the spontaneous contraction stopped (Fig. 4). The increase was not homogeneous; some thread-like structures often showed a rapid initial increase (arrows in Fig. 4A). These structures appeared to be mitochondria, which were stained by a mitochondria marker (i.e., Mitotracker) (Fig. 4B). Interestingly, the increase in the fluorescence of DAF-2 was restricted to an area within the irradiated region, indicating that NO production by the laser was a regional and local event.

Dorsal root ganglion cells

The laser irradiation-induced DAF-2 fluorescence increased in isolated ganglion cells from the dorsal root ganglia. The power of the laser required to induce NO production in ganglion cells was stronger than that in other cell types (5,000–7,700 mJ/cm^2/s v.s. 300–500 mJ/cm^2/s in cardiomyocytes or mast cells). Interestingly, the fluorescence intensity was increased in many punctuate regions, which then spread (Fig. 5).

Hippocampal neurons

A cultured neuron is composed of a central cell body including a nucleus and many cellular processes, which are referred to as axon and/or dendrite. It is well known that there are many thread-like mitochondria in the cellular processes as well as in the cell body. The fluorescence intensity of DAF-2 increased in cultured hippocampal neurons upon laser irradiation (ca. 1,800 mJ/cm^2/s) (Fig. 6). Both the cell body and cellular processes showed an increase. Similarly to dorsal root ganglions, punctuate increases were observed in cultured nerve cells (Fig. 6, white arrows). It is noteworthy that the increase is not linear, but is initially slow (Fig. 6; black arrows), and then rapid (Fig. 6; arrow heads), although significance of the biphasic pattern is yet unknown.

Peritoneal mast cells

Compared to nervous cells, an increase in DAF-2 fluorescence in mast cells was induced by a relatively weak laser (ca. 500 mJ/cm^2/s). The laser initially induced NO production in the granular region, followed by the nuclear region (Fig. 7). The increase in the granular region was speckled. NO production in mast cells may be NO-synthase (NOS)-independent, because some NOS-inhibitors (1 mM L-NAME or 10 μM DPI) did not inhibit the increase in DAF-2 fluorescence (Data not shown).

After laser irradiation (ca 7,000 mJ/cm^2/s, for 3 min), the secretory response to compound 48/80 (a typical stimulant for mast cells) was inhibited, although an increase in intracellular Ca^{2+} was detected by Fluo-3 imaging (data not shown). Interestingly, cells that were locally irradiated (e.g., line scan mode) showed a local inhibition of exocytosis, while exocytosis occurred in non-irradiated regions (Fig. 8). A regional restriction of the effect of laser irradiation on the cell function was also observed in cardiomyocytes, as described above. It is not likely that laser-induced NO diffused freely within the entire cytoplasm.

Inhibition of NO production and photobleaching – Minimal effects of antioxidants

Mast cells were used in this experiment. A stronger laser power caused a higher peak and a more rapid

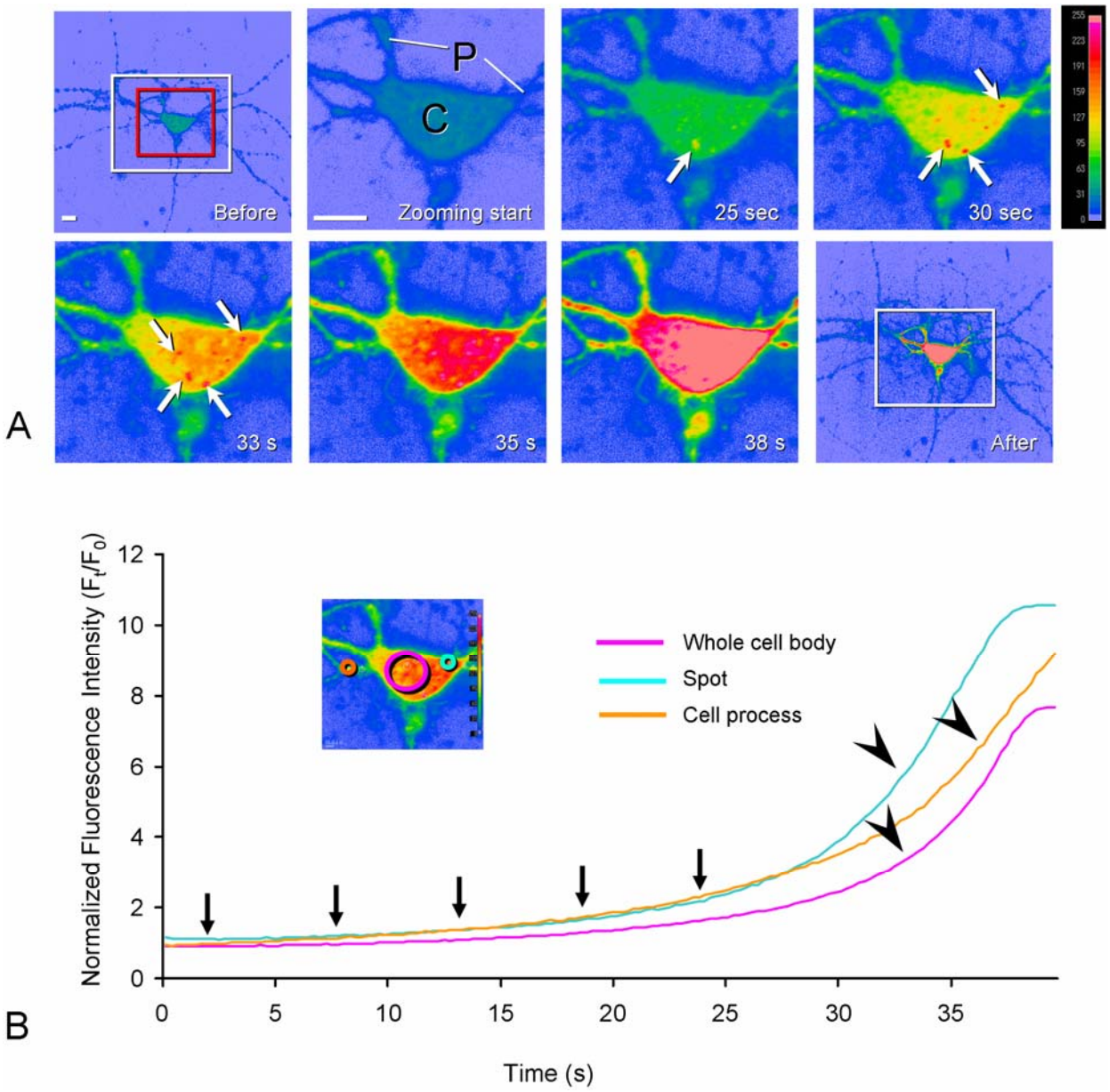

Fig. 6. Cultured hippocampal neuron showing NO production. (A) Pseudocolor images showing the fluorescence intensity of DAF-2. Intense laser radiation at zoom-in (×4) (488 nm; 350→ 1,800 mJ/cm^2/s) induces an increase in DAF-2 fluorescence in the cell body and processes. The irradiated region at zoom-in is outlined by a white rectangle. Zoom-in images (outlined by red rectangle) are smaller than the irradiated area. Spot-like structures show an initial increase (arrows). C: cell body. P: cellular processes. Bar: 10 μm. (B) Time-course of normalized fluorescence intensity (Ft/F0; F0: fluorescence intensity at the start, Ft: temporal fluorescence intensity). Note, the increase was not constant; initially, the increase was slow (black arrows), but after certain period, the intensity increased rapidly (arrow heads).

increase in NO production, and a decrease in laser power was effective in increasing DAF-2 fluorescence intensity (Fig. 9A). Before the experiments, we suspected that intermittent radiation might minimize NO production, but this was not the case. As shown in Figure 9B, laser irradiation at intervals had little effect on the overall process. Regardless whether or not a time interval was used, the increase in DAF-2 fluorescence was proportional to the sum of the irradiation time, although the fluorescence intensity peak was somewhat

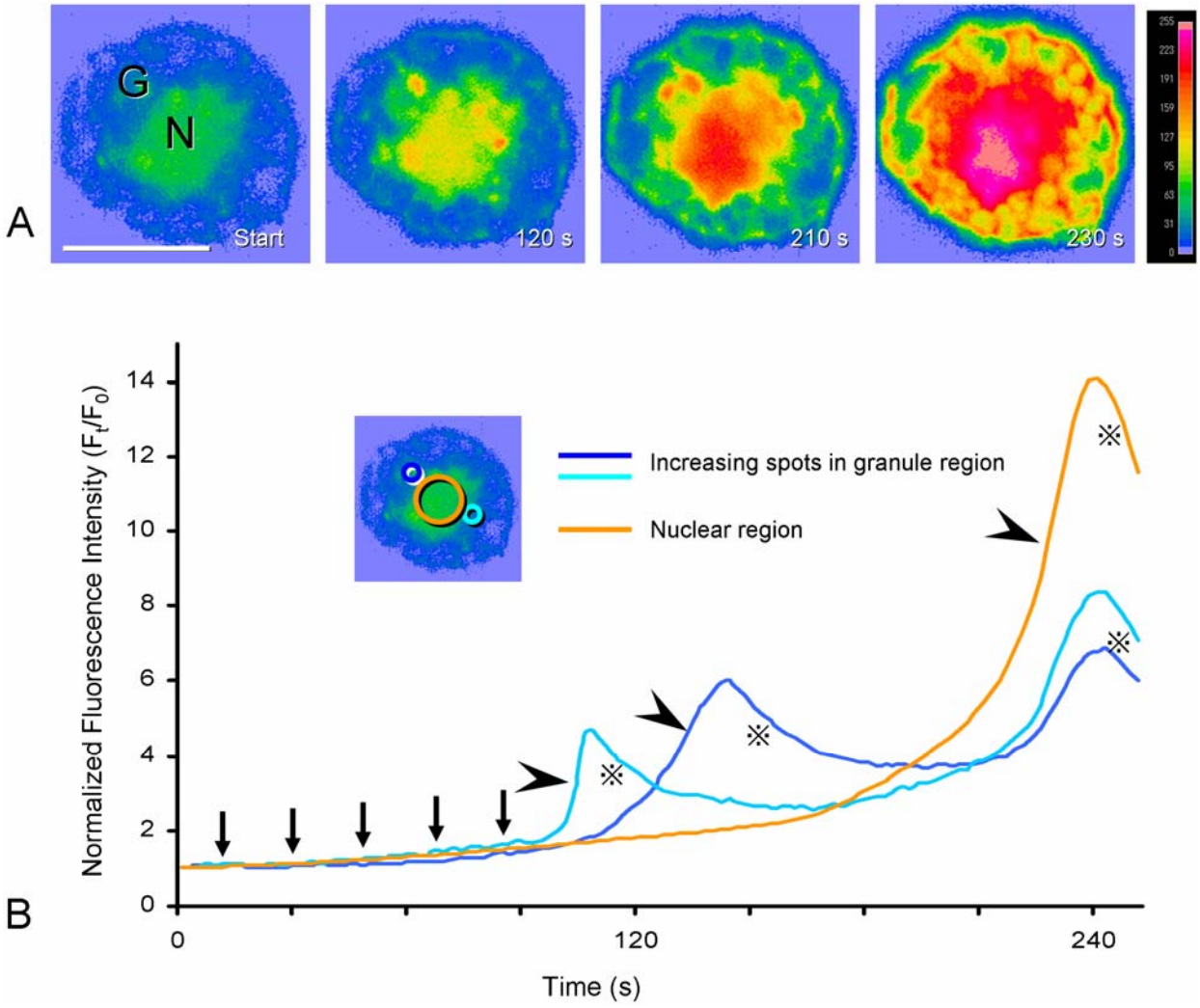

Fig. 7. Peritoneal mast cells showing NO production. (A) Pseudocolor images showing the fluorescence intensity of DAF-2. Laser irradiation (488 nm; 580 mJ/cm^2/s) induced increase in DAF-2 fluorescence in granular regions and the nucleus. N: nucleus. G: peripheral granule region. Bar: 10 μm. (B) Time-course for the changes in fluorescence intensity. Values are normalized (Ft/F0; F0: fluorescence intensity at the start, Ft: temporal fluorescence intensity). Note the biphasic pattern: initial slow (arrows) and late rapid phases (arrow heads). Decline in intensities (※) are considered to be photo-bleaching.

lower when the laser was used intermittently, compared to continuous irradiation. This indicates that the NO-production during laser irradiation is accumulative, and the recovery from the damage during a pause of laser irradiation is negligible. If the laser scanning speed was lowered, the signal/noise ratio improved, while the laser exposure time increased, after which, photodamage was increased.

Substances that have anti-oxidant properties (BSA, vitamin E and melatonin) inhibited the intensity of the DAF-2 peak and delayed the time course, only when the laser power was weak (Fig. 10A). These had no effect on the bleaching of Indo-1 (Fig. 10B) (data on melatonin not shown).

Measurement of free radicals with a non-specific indicator

Because light or laser induces the production of various free radicals and/or reactive oxygen species, except for NO, imaging with other free radical indicators (e.g., DCF) might be used in terms of monitoring photo-damage. However, the increase in fluorescence of DCF was quite rapid, even when the laser power was

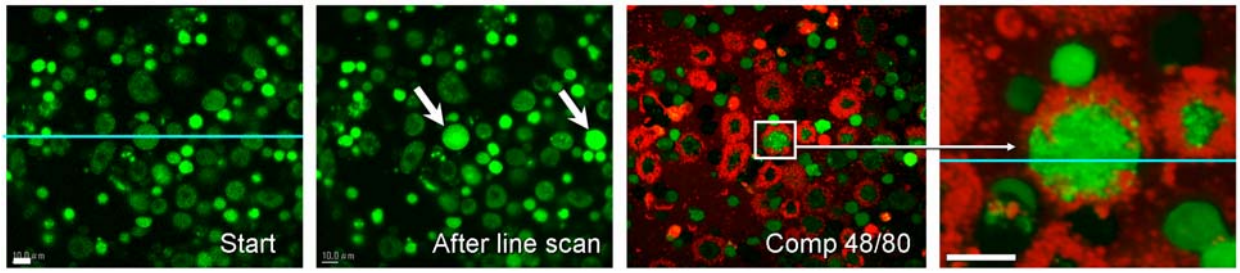

Fig. 8. Peritoneal mast cells irradiated by laser of line-scan mode. Mast cells were loaded with DAF-2 (colored by green), and exocytotic granules were stained with SFRM-B (red). Light-blue line indicates linear scanning of laser beam (488 nm; 165,000 mJ/cm^2/s). Two cells were exposed to an equatorial plane, and DAF-2 intensity increased within a few seconds (white arrows). Thereafter, the cells were stimulated with compound 48/80 (ca. 10 μM). Normally, exocytosis occurs in all directions, and exocytosed granules appear doughnut-like. However, exocytosis was inhibited at the irradiated plane of the line-scanned cells. Bar: 10 μm.

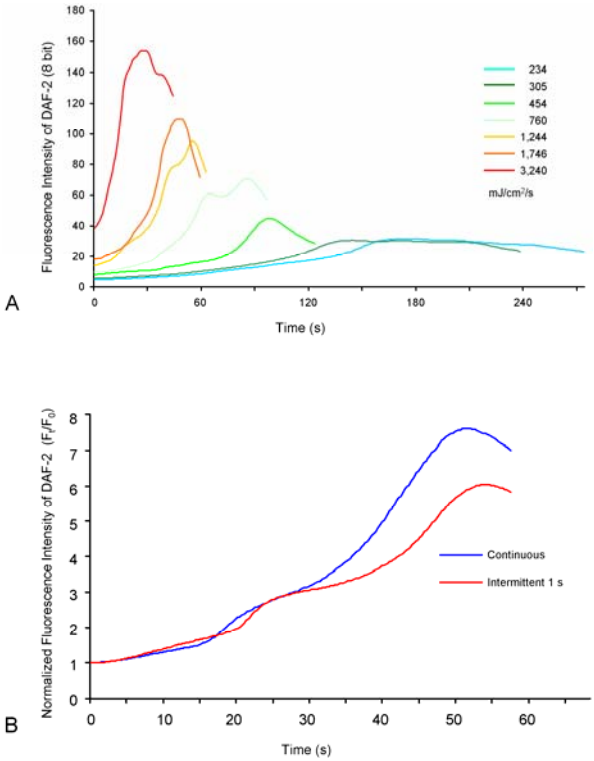

Fig. 9. Effects of power and duration of laser irradiation on DAF-2 intensity in mast cells. (A) Mast cells were loaded with DAF-2, and irradiated by a blue laser at a different power of a blue laser (488 nm). (B) Time-course for normalized fluorescence intensity of DAF-2 (Ft/F0; F0: fluorescence intensity at the start, Ft: temporal fluorescence intensity) under continuous or intermittent (irradiation for 1/4 sec and pause for 3/4 s) irradiation (488 nm; 1,280 mJ/cm^2/s). Time in the horizontal axis represents the sum of the actual irradiation time.

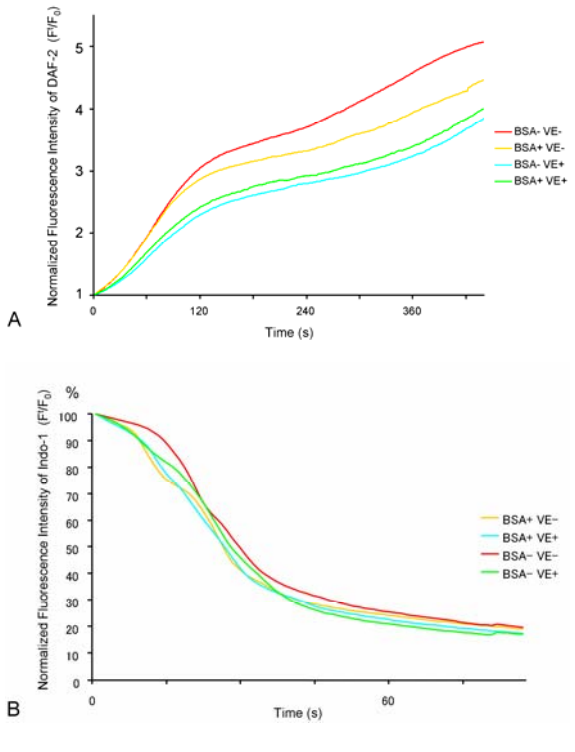

Fig. 10. Effects of BSA and vitamin E on laser-induced increase of DAF-2 intensity and photobleaching of mast cells. (A) Time courses for normalized DAF-2 intensity (Ft/F0; F0: fluorescence intensity at the start, Ft: temporal fluorescence intensity) with or without BSA (5%) and/or vitamin E (200 μM) in perfusion solution. Mast cells were exposed to a blue laser (488 nm; 700 mJ/cm^2/s). (B) Time courses of Indo-1 intensity (percent of Ft/F0; F0: fluorescence intensity at the start, Ft: temporal fluorescence intensity) with or without bovine serum albumin (5%) and/or vitamin E (200 μM) in the perfusion solution. Mast cells were exposed to a UV-laser (351 nm; 120 mJ/cm^2/s, which was a rough relative value).

minimized to the utmost limit. This indicates that, in bioimaging experiments, the irradiation by the light or a laser induces the formation of free radicals, even when the light or the laser is faint, and that DCF was too sensitive to permit photodamage to be assessed.

Discussion

In fluorescence bioimaging experiments, the exciting laser power or the light intensity should be minimized to avoid the photodamage and photobleaching by free radicals. A number of intracellular signalling mechanisms are perturbed by radicals, and bleaching results in difficulties associated with long-term observation. To acquire a quality of image sufficient to evaluate (sub) cellular changes, specimens must be extensively excited with the light or laser, although in such cases, the possibility of photodamage to living cells is often ignored. The trade-off between the photodamage (photobleaching) and the good image acquisition is an empirical issue. In the present study, we proposed the quantitative estimation of photodamage by DAF-2; a type of bioassay for the photodamage. This procedure is recommended as a preliminary test to evaluate a possible photodamage.

A monitor showing the numerical value of the laser power is introduced in most confocal laser microscopes, but the value does not linearly reflect the laser energy. Thus an equation needs to be developed to solve this, as was done in the present study. However, a laser power meter that measures the actual power of laser (e.g., thermo couple type) is too expensive, while values obtained by low-cost silicon types are relatively inaccurate. In addition, we were able to estimate only the power of the radiation at the objective lens, but no objective procedure is available for estimating laser power in actual cells and tissues. After the increase in DAF-2 fluorescence intensity, the beating of cardiomyocytes and exocytosis in mast cells were damaged, indicating that the production of NO detected by a fluorescence imaging interferes with some physiological responses in various cells. Monitoring susceptibility to laser irradiation with DAF-2 in fluorescence imaging is convenient and practical, to determine the extent of such photodamage.

In the present findings concerning increased levels of NO, nervous cells were found to be more robust against laser radiation, compared with cardiomyocytes or mast cells. Susceptibility with laser irradiation varies among different cells. This indicates that there is no standard value of laser power for producing minimal photodamage. The exact mechanism of the differences in photosusceptibility of various cells is unclear. The present examination indicated that mitochondria are correlated with laser-induced NO production, and therefore, the photosusceptibility of a cell can depend on the nature of the mitochondria of the cell. Although NOS in mitochondria can produce NO (Elfering et al., 2002), the increase in NO levels during laser irradiation was NOS-independent. Therefore differences in NOS activity cannot be used as an index. Some mitochondrial proteins are sensitive to visible light (Hollis et al., 2003), and as a result, differences in photosensitive proteins in mitochondria may result in various photosusceptibility. In addition, some photosensitive substances (e.g., porphyrins in the rodent Harderian gland) in the cytoplasm can be correlated with light/laser-induced NO production.

Anti-oxidative substances are used for photoprotection in dermatological therapy (Anstey, 2002), but their use is empirical, in attempts to minimize photodamage or photobleaching in experimental laboratories. The addition of BSA to extracellular perfusion solutions increases the viability of cells, and BSA contains multiple S-S binding sites which may play a role as an anti-oxidant. Anti-oxidants improve the function of isolated mitochondira (Brewer et al., 2004). Therefore, we anticipated that anti-oxidative substances might inhibit the NO production and photobleaching during laser irradiation. However, in the present study, we confirmed that extracellular anti-oxidants had only minimal effects on the intracellular NO-production, only when laser power was quite low (ca. <500 mJ/cm^2/s). Vigorous anti-oxidative substances (e.g., sodium azide, which is often used to protect against photobleaching in immunohistochemistry in chemically fixed tissues or cells) disturb various signalling systems in living mitochondria. We conclude, therefore, that there are few novel materials that are capable of reducing the photodamage or photobleaching in the fluorescence bioimaging in living tissues or cells. To reduce photodamage and photobleaching, it is essentially necessary 1) to minimize laser power and 2) to scan as rapidly as possible.

In conclusion, to assess the critical laser power in fluorescence bioimaging, the effective monitoring of photodamage is necessary, and photosusceptibility varies among different cells. To this end, the DAF-2 imaging method can be a useful and practical tool.

Acknowledgments

This work was supported by research grants from the Ministry of Education, Culture and Science of Japan (Y.S.; 17390053) and from the Promotion and Mutual Aid Corporation for Private Schools of Japan. A portion of this work was performed at the Advanced Medical Science Center of Iwate Medical University, with its financial support.

Received Febrary 26, 2006; revised version accepted July 28, 2006.

References

Anstey, A.V. (2002). Systemic photoprotection with alpha-tocopherol (vitamin E) and beta-carotene. Clin. Exp. Dermatol., 27: 170–176.

Berridge, M.J., Bootman, M.D. and Roderick, H.L. (2003). Calcium signalling: dynamics, homeostasis and remodelling. Nat. Rev. Mol. Cell Biol., 4: 517–529.

Brewer, G.J., Jones, T.T., Wallimann, T. and Schlattner, U. (2004). Higher respiratory rates and improved creatine stimulation in brain mitochondria isolated with anti-oxidants. Mitochondrion, 4: 49–57.

Cui, Z.J., Habara, Y. and Satoh, Y. (2000). Photodynamic modulation of adrenergic receptors in the isolated rat hepatocytes. Biochem. Biophys. Res. Commun., 277: 705–10.

Cui, Z.J. and Guo, L.L. (2002). Photodynamic modulation by Victoria Blue BO of phenylephrine-induced calcium oscillations in freshly isolated rat hepatocytes. Photochem. Photobiol. Sci., 1: 1001–1005.

Elfering, S.L., Sarkela, T.M. and Giulivi, C. (2002). Biochemistry of mitochondrial nitric-oxide synthase. J. Biol. Chem., 277: 38079–86.

Kawata, M., Matsuda, K., Nishi, M., Ogawa, H. and Ochiai, I. (2001). Intracellular dynamics of steroid hormone receptor. Neurosci. Res., 40: 197–203.

Kojima, H., Nakatsubo, N., Kikuchi, K., Kawahara, S., Kirino, Y., Nagoshi, H., Hirata, Y. and Nagano, T. (1998). Detection and imaging of nitric oxide with novel fluorescent indicators: diaminofluoresceins. Anal. Chem., 70: 2446–53.

Konno, D., Ko, J.A., Usui, S., Hori, K., Maruoka, H., Inui, M., Fujikado, T., Tano, Y., Suzuki, T., Tohyama, K. and Sobue, K. (2002). The postsynaptic density and dendritic raft localization of PSD-Zip70, which contains an N-myristoylation sequence and leucine-zipper motifs. J. Cell. Sci., 115: 4695–706.

Miyata, S., Haneda, T., Osaki. J. and Kikuchi, K. (1996). Renin-angiotensin system in stretch-induced hypertrophy of cultured neonatal rat heart cells. Eur. J. Pharmacol. 307: 81–88.

Mori, S., Saino, T. and Satoh, Y. (2000). Effect of low temperatures on compound 48/80-induced intracellular Ca^{2+} changes and exocytosis of rat peritoneal mast cells. Arch. Histol. Cytol., 63: 261–70.

Nahorski, S.R., Young, K.W., John Challiss R.A. and Nash, M.S. (2003). Visualizing phosphoinositide signalling in single neurons gets a green light. Trends. Neurosci., 26: 444–452.

Preiser, J.C., Reper, P., Vlasselaer, D., Vray, B., Zhang, H., Metz, G., Vanderkelen, A and Vincent, J.L. (1996). Nitric oxide production is increased in patients after burn injury. J. Trauma, 40: 368–71.

Waguri, S., Dewitte, F., Le Borgne, R., Rouille, Y., Uchiyama, Y., Dubremetz, J.F. and Hoflack, B. (2003). Visualization of TGN to endosome trafficking through fluorescently labeled MPR and AP-1 in living cells. Mol. Biol. Cell, 14: 142–155.